

*Journal of*  
***Mechanics of***  
***Materials and Structures***

**STATISTICAL STRENGTH OF A TWISTED FIBER BUNDLE: AN  
EXTENSION OF DANIELS EQUAL-LOAD-SHARING PARALLEL  
BUNDLE THEORY**

Pankaj K. Porwal, Irene J. Beyerlein and S. Leigh Phoenix

***Volume 1, N° 8***

***October 2006***



mathematical sciences publishers

## STATISTICAL STRENGTH OF A TWISTED FIBER BUNDLE: AN EXTENSION OF DANIELS EQUAL-LOAD-SHARING PARALLEL BUNDLE THEORY

PANKAJ K. PORWAL, IRENE J. BEYERLEIN AND S. LEIGH PHOENIX

In this work, we extend the statistical strength model of Daniels for a parallel fiber bundle to a twisted bundle with an ideal helical structure. The bundle is clamped at each end in such a way that it has no slack fibers in the unloaded state. The fibers are linearly elastic and continuous, and have random strengths following a Weibull distribution with Weibull shape parameter  $\rho$ . We calculate the stress redistribution from failed to surviving fibers according to a twist-modified equal load sharing (TM-ELS) rule, introduced here. The effect of the twist is modeled analytically by two approaches, one called *geometrical averaging*, in which the fiber helix angles are averaged, and the other called *statistical averaging*, in which the fiber failure probabilities are averaged. In both probability models, the bundle strength distributions remain asymptotically Gaussian, as in Daniels' original model; however, the associated mean and standard deviation are additionally altered by the surface twist angle. To validate these theories, a Monte Carlo model is developed to simulate fiber break initiation and progression within a cross-sectional plane under tension. For all values of surface twist angle  $\alpha_s$ ,  $\rho$  and bundle size studied, the simulated strength distributions are shown to be strongly Gaussian. Transitions in failure mode from diffuse, across the bundle cross-section, to localized near the center of the bundle occur when  $\alpha_s$  and  $\rho$  increase and the bundle size decreases, in spite of application of a diffuse-type loading sharing rule, TM-ELS. Both analytical models provide similar results which are in excellent agreement with the simulated results. For the most part, we consider the bundle to be short enough that interfiber friction plays no role in the stress redistribution. However, to demonstrate its importance in long bundles, we mimic the effects of interfiber friction by considering a chain of such bundles where the bundle length is chosen to approximate the characteristic length of unloading around breaks.

### 1. Introduction

Yarns, ropes, and cables, generically called twisted mechanical structures, have been used for centuries as load-bearing structures. When fabricated from ultrastrong, high-performance polymer-based or carbon-based fibers, such as Kevlar, PBO, graphite, and even carbon nanotubes (see, for example, [Vigolo et al. 2000; Zhang et al. 2004]) such structures can be made with superior strengths and can possibly be used in many technically advanced aerospace and defense applications. Like traditional fibers, such as wool, cotton and polyester, these advanced fibers exhibit a substantial variation in strength as well

---

*Keywords:* twisted fiber bundle or yarn, Monte Carlo simulation, statistical strength, twist modified equal load sharing (TM-ELS), ideal helical structure, interfiber friction, chain-of-bundles model.

The authors gratefully acknowledge the support of the Science and Technology-based Distinguished Student Award provided to graduate student Pankaj K. Porwal by Los Alamos National Laboratory (LANL) and the support of a LANL-directed Research and Development project (No. 20030216) provided to IJB. This work has been supported in part under the *Institute for Future Space Transport*, a NASA University Institute funded under Cooperative Agreement NCC3-994.

as size (length and number of fibers) effects. Consequently the strength of the twisted structure made from such fibers will also exhibit similar characteristics, although it may be much weaker depending on the extent of variability and the stiffness of the fibers. Thus, there is a need for structural strength predictions, particularly in the high reliability regime, that is, only one failure out of thousands or millions of specimens under a design load. In other words, an average strength determined from a few tests will not be sufficient. Such predictive capability, however, is not in place for these twisted structures.

In these structures, the local material strengths vary from point to point and from fiber to fiber within the bundle. As a consequence, the failure processes can be quite random and the strengths can statistically vary among twisted bundles of otherwise identical descriptions. As the bundle volume increases (either in diameter or length) the likelihood of finding a weak region or defect that can lead to failure will increase as well, leading to a lower average strength among many specimens. Fiber strengths are commonly described by the Weibull distribution, an empirical statistical model that was built upon weakest-link concepts [Phoenix and Beyerlein 2000]. However, the strength distribution and size effect for a twisted fiber bundle are generally more complicated and unknown.

These twisted structures are also heterogeneous in microstructure. To see this, envision fibers in layers following concentric helical paths about the central axis of the fiber ‘bundle’ (for example, yarn, rope, cable) with helical angles varying from zero, for the central fiber, to  $\alpha_s$ , for fibers at the surface. Under the action of an applied load, the stresses or strains sustained by individual fibers differ depending on their helical angle with respect to the loading direction and the angles of the surrounding fibers. In addition, their stresses will depend on the actual distribution of neighboring fiber breaks.

Unlike the initial or elastic modulus, the strength of a heterogeneous material cannot be predicted by a rule-of-mixtures type calculation. Strength is best predicted by considering failure mechanisms involving various initiation phenomena and subsequent propagation behavior to catastrophic collapse. The two primary mechanisms in a twisted fiber bundle are fiber failure and fiber slipping (for example, unraveling), which may occur simultaneously. This interplay of failure mechanisms is a favorable situation, which can theoretically lead to optimal strengths without compromising ductility.

In this work, we develop analytical models for bundle strength based only on the first mechanism, fiber breaks and load redistribution. They allow for a stochastic progression of fiber breaks within a cross-sectional plane of an ideal helical structure. Under the initial application of strain or stress, breaks occur first in the weakest or most highly stressed fibers. As the stress level increases, breaks increase in number until an unstable pattern of breaks and the maximum stress that can be sustained, is achieved.

To validate the simplifying assumptions made in the analytical models, a Monte Carlo computational model is developed. This computational model simulates more accurately the ‘true’ failure progression in many replications, sufficient for generating empirical statistical strength distributions. This useful tool provides insight into the mathematical form of the bundle strength distributions, characteristics of the failure modes, and dependencies on statistical fiber strength properties and surface twist angle,  $\alpha_s$ . In this work, both the Monte Carlo and analytical models consider Weibull fiber strengths and a nonlocalized load sharing rule among broken and intact fibers called the twist-modified equal load sharing (TM-ELS) rule. In TM-ELS, failed fibers carry zero stress and surviving fibers share the applied bundle load but carry individual stresses depending on their radial positions in the bundle. As a consequence, fiber breaks will propagate based not only on their strengths and the total number of breaks, but on their helix angle as well. Like the conventional ELS rule, no direct enhancements result from the relative proximity of

one break to another. Pure ELS is well known to apply to dry bundles of parallel fibers when there is negligible friction between the fibers, which causes load build-up from the fiber ends to be rather inefficient. For a twisted bundle, however, we show that in spite of the TM-ELS assumption, the Monte Carlo model forecasts transitions in failure mode from ductile-like to brittle-like due to the twist angles and fiber strength variation.

While very important, incorporating the effects of friction and slipping is beyond the scope of the current work and will be considered in a sequel. Nonetheless, as a preview of the expected behavior we perform a simple chain-of-bundles calculation, using results of [Alexander 1952] for the stress recovery length around a fiber discontinuity in terms of yarn tension and twist. However, in the actual yarn the stress transfer length around a broken fiber depends on its radial position because the radial pressure distribution is nonuniform.

## 2. Theoretical background

Most theories for yarns, ropes, and cables operate within a deterministic strength paradigm with the goal of determining the optimal surface twist angle at which the highest bundle strength is achieved. In fact, fiber manufacturers often apply twist to varying degrees (not necessarily the same from one lot to the next) to determine fiber strength to meet some acceptance criteria or minimum standard. The optimal twist angle is generally related to a single-valued fiber strength, fiber diameter and length, and the magnitude of frictional forces in shear acting along fibers to resist sliding. For an excellent summary of the earlier, classical theoretical and experimental works, we refer the reader to [Hearle et al. 1969]. Other more recent attempts in this category, including work on impregnated yarns, can be found in [Naik et al. 2001], where the strength of impregnated yarn was estimated using an effective shear traction and fiber obliquity factor.

On the other hand, most statistical strength models treat a parallel array of fibers rather than a twisted bundle. These models generally focus on the influence of fiber strength, bundle length, bundle size, fiber packing, and interface properties, in the case when matrix is present in the parallel fiber bundle. For a recent review of these parallel bundle theories, we refer the reader to [Phoenix and Beyerlein 2000]. Among these we mention only the classical theory of Daniels [1945], which is relevant to this work. Through a long and complicated proof, Daniels showed that when the load from fiber breaks is redistributed equally among the remaining intact fibers (ELS), the strength of a large bundle asymptotically approaches a Gaussian distribution. He derived expressions for the asymptotic mean  $\mu_D$  and standard deviation  $\gamma_D$  as a function of the underlying strength distribution of the fibers and bundle size in terms of number of fibers.

There are, however, a few notable statistical strength theories for twisted fiber bundles [Phoenix 1979; Pan 1993]. Although using different approaches, they both have extended Daniels' parallel bundle theory. Phoenix [1979] in particular studied the influence of slack as a result of incomplete migration, that is, the deviation of fibers from an ideal helical path, that occurs after the twisting process. He proposed a statistical model for random fiber slack, which has two characteristic parameters reflecting the extent and uniformity of the migration process, and applied it to an ideal helical structure where the fiber strength itself followed a Weibull distribution. An asymptotically Gaussian distribution for the strength of the twisted yarn was argued to apply, as in Daniels' case, and the associated mean and standard deviation

were derived. We compare the results of [Phoenix 1979] to that of the present work. Pan [1993] derived and directly applied an orientation efficiency factor to Daniels' mean  $\mu_D$  and standard deviation  $\gamma_D$  to account for the effect of an average twist. Up to now, twisted bundle strength studies have not used Monte Carlo simulation to investigate the nature of the yarn strength distribution or to validate the Gaussian form of the distribution, which had been assumed upfront to apply to twisted structures and in fact many other structures outside of the parallel ELS bundle.

### 3. Modeling approach

**3.1. Parallel bundle.** Our models for the strength of a twisted bundle will build upon Daniels' well-known theory for a parallel ELS bundle. His model is briefly reviewed here.

Daniels [1945] considered  $n$  parallel fibers that are evenly clamped at each end and have the same cross-sectional area  $A$  and linear elastic constitutive law with Young's modulus  $E_f$ . The fiber strengths  $X_1, X_2, \dots, X_n$  (in units of stress) are independent and identically distributed (i.i.d.) random variables following a cumulative distribution function (cdf)  $F(s)$ ,  $s \geq 0$ , where  $s$  is the stress in the fiber along the direction of loading. When the fibers are parallel to the direction of loading,  $s$  is also the axial stress in the fibers. The corresponding strain to failure of fiber  $i$ ,  $\xi_i$ , is simply  $\xi_i = X_i/E_f$ .

A nominal stress  $\sigma$  is uniformly applied to this  $n$ -sized bundle, and as  $\sigma$  is increased, the fibers start to break whenever and wherever the fiber stress exceeds the fiber strength. Due to the strength variation, fiber breaks tend to initiate and spread in a random manner. According to the ELS rule of Daniels' model, when a fiber breaks, its lost load is instantaneously redistributed in equal portions to all surviving fibers. Consequently, the individual axial stresses, denoted here as  $s$ , in the remaining intact fibers will be equal, and will be higher than  $\sigma$  for the bundle. If  $N_b$  is the current number of breaks in the bundle, then according to ELS,  $s$  is

$$s = \left( \frac{n}{n - N_b} \right) \sigma.$$

The strength of the bundle  $S$  is the maximum stress borne by the bundle, and is given by

$$S = \max \left\{ X_{1,n}, \left( \frac{n-1}{n} \right) X_{2,n}, \dots, \left( \frac{1}{n} \right) X_{n,n} \right\},$$

where  $X_{1,n} \leq X_{2,n} \leq \dots \leq X_{n,n}$  are the order statistics of the strengths of the  $n$  fibers. Daniels proved that  $S$  asymptotically follows a Gaussian (that is, normal) distribution, with probability density function (pdf)  $g_n(s)$  given by

$$g_n(s) = \frac{1}{\sqrt{2\pi}\gamma_D^2} \exp \left\{ -\frac{(s - \mu_D)^2}{2\gamma_D^2} \right\}, \quad (1)$$

where  $\mu_D$  is the mean and  $\gamma_D$  is the standard deviation of the bundle strength.

In general the bundle can be loaded in a stress-controlled or strain-controlled manner. In the latter, with increasing strain  $\epsilon_y$  on the bundle, the resulting bundle stress fluctuates randomly. For a large bundle (that is,  $n \rightarrow \infty$ )  $\sigma(s)$ , the nominal bundle stress as a function of  $s$  asymptotically approaches the function  $\mu(s)$  given by

$$\mu(s) = s[1 - F(s)], \quad s \geq 0.$$

The  $\mu_D$  in Equation (1) is the maximum of  $\mu(s)$ , formally called the asymptotic mean strength, and is

$$\mu_D = \max_s \{\mu(s) : s \geq 0\}. \tag{2}$$

$\mu(s) = \mu_D$  occurs when  $s = s^*$ , that is,  $s^* = \{s : \mu(s) = \mu_D\}$ . The variance function for the bundle stress is given by

$$\Sigma(s) = s^2 F(s)[1 - F(s)], \quad s \geq 0,$$

and the asymptotic standard deviation  $\gamma_D$  of the bundle strength is

$$\gamma_D = \frac{s^*}{\sqrt{n}} \sqrt{F(s^*)[1 - F(s^*)]}. \tag{3}$$

Note that the asymptotic value  $\mu_D$  is independent of  $n$ . Smith [1982] derived a correction factor for  $\mu_D$  that depends on  $n$  to improve the accuracy of  $\mu_D$  for relatively small bundles. The correction factor is given by

$$\Delta_n^* = \frac{0.996}{n^{2/3}} \left\{ \frac{F'(s^*)^2 s^{*4}}{2F'(s^*) + s^* F''(s^*)} \right\}^{1/3}, \tag{4}$$

where prime means derivative. This factor is added to  $\mu_D$ , to yield  $\mu_D^* = \mu_D + \Delta_n^*$ . Later, McCartney and Smith [1983] derived an improved asymptotic standard deviation of bundle strength, which is

$$\gamma_D^* = \gamma_D \sqrt{1 - 0.320 \left(\frac{\Delta_n^*}{\gamma_D}\right)^2}.$$

In the remainder of this work,  $F(T)$  for fiber strength will follow a Weibull distribution

$$P(X \leq T) = F(T) = 1 - \exp \left\{ -\left(\frac{T}{\sigma_\delta}\right)^\rho \right\},$$

where  $T$  is fiber stress along its axis, and  $\sigma_\delta$  and  $\rho$  are the Weibull scale and shape parameters, respectively. The corresponding  $\mu_D$  and  $\gamma_D$  in Equations (2) and (3) are

$$\mu_D = \sigma_\delta (\rho e)^{-1/\rho}, \quad \gamma_D = \left(\frac{\sigma_\delta}{\sqrt{n}}\right) \rho^{-1/\rho} \sqrt{e^{-1/\rho}(1 - e^{-1/\rho})}, \tag{5}$$

and the correction factor in Equation (4) becomes

$$\Delta_n^* = \frac{0.996 \mu_D}{n^{2/3}} \left(\frac{e^{2/\rho}}{\rho}\right)^{1/3}. \tag{6}$$

The improved  $\mu_D^*$  and  $\gamma_D^*$ , according to [Smith 1982; McCartney and Smith 1983], become

$$\mu_D^* = \mu_D \left\{ 1 + \frac{0.996}{n^{2/3}} \left(\frac{e^{2/\rho}}{\rho}\right)^{1/3} \right\}, \quad \gamma_D^* = \gamma_D \sqrt{1 - 0.317 \left(\frac{\mu_D}{\gamma_D}\right)^2 \left(\frac{e^{2/\rho}}{n^2 \rho}\right)^{2/3}}. \tag{7}$$

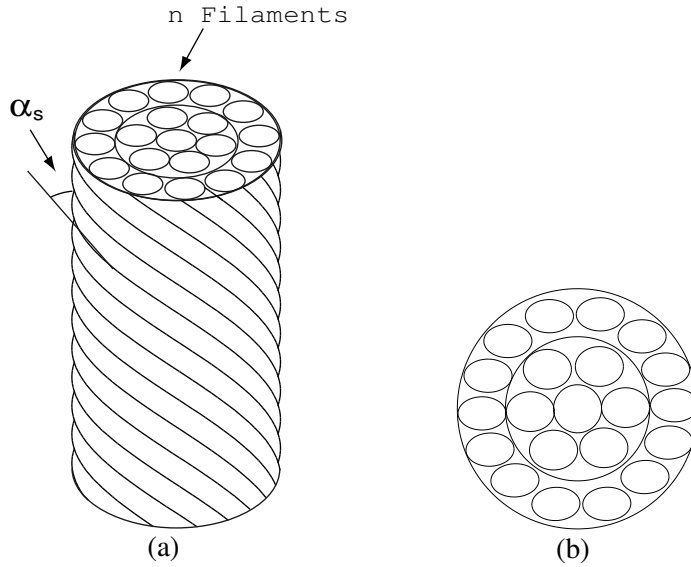


**Figure 1.** (a) Yarn segment and (b) Cross-sectional view of concentric packing.

**4. Strength of twisted fiber bundles**

**4.1. Helical yarn geometry.** The most commonly analyzed geometry of a twisted fiber bundle or yarn is the one in which the fibers lie in concentric cylindrical layers. Within each layer, fibers follow ideal helical paths with the same helix angle, as shown in Figure 1a, but the angle differs from layer to layer. In this idealization, fibers in different layers necessarily must have different lengths to be strain-free yet without slack. This implies that between two yarn cross-sections, fibers (other than the center fiber) will have lengths (when straight) equal to their helical path lengths, and thus, will be longer than the distance between these cross-sections.

Consider an ideal helical structure with  $l$  layers, numbered  $1, \dots, k, \dots, l$ , of fibers with diameter  $d_f$ . The  $l$  layers have respective helix angles  $\alpha_1, \dots, \alpha_k, \dots, \alpha_l$ , and are located at radii  $r_1, \dots, r_k, \dots, r_l$  from the center of the bundle axis. Note that  $r_k$  is the distance from the center of the yarn to the center of the fiber in layer  $k$ . Also the radius of the yarn,  $R$  is taken as  $r_l$ .

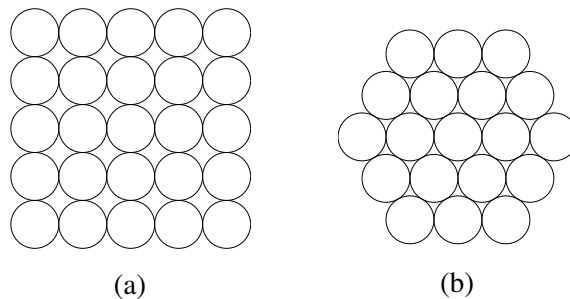


**Figure 2.** Square and hexagonal packing.

Note also that in the cross-sectional view, the fibers are arranged in concentric layers, which we call concentric packing. Concentric packing is different from other commonly used fiber packing models, such as square packing [Figure 2a](#) or hexagonal packing [Figure 2b](#). We also assume that the gap between the layers is negligible compared to the diameter of the fiber. Under these assumptions  $r_k$ , approximately becomes  $r_k \approx (k - 1)d_f$ . If we also assume complete filling of the layers, that is, a fiber will occupy any void in a concentric layer that is large enough to accommodate it, the number of fibers in the  $k^{\text{th}}$  concentric layer,  $n_k$ , is approximately

$$n_k \approx \left\lfloor \frac{2\pi r_k}{d_f} \right\rfloor \approx 2\pi(k - 1), \quad \text{for } k \geq 2, \tag{8}$$

where  $n_1 = 1$  and where  $\lfloor x \rfloor$  means the largest integer less than or equal to  $x$ . As expected,  $n_k$  does not depend on  $d_f$ . The total number of fibers in the bundle  $n$  with  $l$  layers is  $n = n_1 + \dots + n_l$ , but can be approximated as  $n \approx 1 + \pi(l - 1)l$ .

As illustrated in [Figure 1a](#), the helix angle of the outer layer  $\alpha_l$  is especially important and is denoted as  $\alpha_s$ , the surface helix angle. From the yarn twisting process, the helix angle  $\alpha_k$  for concentric layer  $k$  depends on its radius  $r_k$  (being approximately proportional to it) and the surface helix angle,  $\alpha_s$ . From the geometry of the helix illustrated in [Figure 3](#) we have

$$\alpha_k = \tan^{-1} \left( \frac{2\pi r_k}{h} \right), \quad \alpha_s = \tan^{-1} \left( \frac{2\pi R}{h} \right),$$

where the second equation is for the surface layer, located at  $r_l = R$ . Here  $h$  is the height, along the yarn axis, of one turn of twist [Figure 3](#).

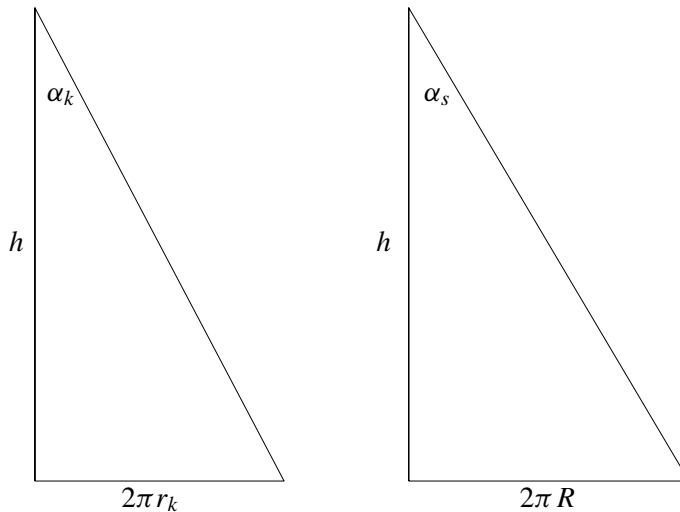


**Figure 3.** The variation of helix angle.

We assume that all layers have the same axial height of one turn of twist,  $h$ , which applies when there is no initial tensile strain or slack in any fiber. Thus,

$$\alpha_k = \tan^{-1} \left( \frac{r_k \tan \alpha_s}{R} \right) \quad (9)$$

in terms of  $\alpha_s$ . In later calculations we will need  $\alpha_{f,i}$ , the helix angle for an individual fiber  $i$ . Let  $\mathfrak{S}_k$  be the set of fibers in layer  $k$ , then  $\alpha_{f,i}$  can be defined as

$$\alpha_{f,i} = \alpha_k, \quad i \in \mathfrak{S}_k \quad \text{and} \quad k = 1, \dots, l.$$

We note that this ideal twisted structure is not common in practice. In a long untwisted yarn all fibers begin with equal lengths, and thus, accomplishing the varying path lengths in different layers during twisting under tension must lead to varying slack or compression in some fibers and uneven strains in others. The yarn attempts to equalize its fiber lengths by the phenomenon called migration. Over a yarn length segment less than or equal to some modest multiple of the yarn diameter, fibers stay within their layer, that is, they do not ‘migrate’. Beyond this length scale, fibers ‘migrate’ to different layers to equalize fiber lengths. If migration is incomplete, there will exist some slack visible as buckling in the fibers due to inefficient migration of fibers, which can lead to inefficiencies in the bundle load-carrying capacity and reductions in strength [Phoenix 1979].

In this paper, we do not model specifically the process of migration. It is assumed that it is complete so that an ideal helical structure is achieved over some bundle length suitable for analysis. Study of the effects of incomplete migration beyond that considered already in [Phoenix 1979] will be left for future work.

**4.2. Transformation of strains.** In this work, we frequently need to transform fiber strains between the individual fiber axis and the bundle axis along which the load is applied. The relationship between the applied bundle strain,  $\epsilon_y$ , and the axial strain,  $\epsilon_f$ , in a fiber of layer  $k$  is taken from basic yarn mechanics [Hearle et al. 1969] and is given by

$$\epsilon_f(\alpha_k) = \epsilon_y(\cos^2 \alpha_k - \nu \sin^2 \alpha_k). \quad (10)$$

In the above,  $\nu$  is the Poisson’s ratio of the yarn. For simplicity we assume  $\nu = 0$ , and thus, neglect any changes in the radial dimension of the yarn under axial loading.

**4.3. Twist-modified equal load-sharing (TM-ELS) rule.** In the case of a parallel fiber bundle, ELS is straightforward and does not violate any of the equilibrium conditions. To modify ELS to apply to a twisted bundle, we simplify the problem greatly by satisfying load equilibrium conditions only in the yarn axis direction. Our general scheme is to model the failure process as progressing in discrete steps  $t = 0, 1, 2, \dots$  in the following way:

- (i) in any particular step,  $t$ , the axial stresses of the surviving fibers are calculated and then compared with the assigned fiber strengths  $X_i$  (as in the case of a parallel fiber bundle);
- (ii) from this comparison, any fiber whose axial stress exceeds its assigned strength is considered breaking in this step. The pre-break stress components in these fibers are resolved along the bundle axis;

- (iii) these resolved components are then redistributed equally to the stress components of the surviving fibers also acting along the yarn axis, and the stresses of these survivors acting along their own respective axes are recalculated;
- (iv) the stresses in these newly broken fibers are then set to zero.

Formulating this approach mathematically, at step  $t$  we denote the stress in fiber  $i$  acting along its own axis (not the yarn axis) as  $T_{f,i}^{(t)}$  as in (i) in the above.  $T_{f,i}^{(t)}$  is considered as composed of two components: The first is the stress carried by the fiber  $T_{f,i}^{\epsilon(t)}$  due to the applied load as if all the fibers are intact and the second component is the sum of the additional stress portions inherited from the broken fibers  $T_{f,i}^{r(t)}$ . Summing these, for fiber  $i$  we have

$$T_{f,i}^{(t)} = \begin{cases} T_{f,i}^{\epsilon(t)} + T_{f,i}^{r(t)}, & \text{for } T_{f,i}^{(t)} < X_i, \\ 0, & \text{otherwise,} \end{cases}$$

where  $X_i$  is its tensile strength. From Equation (10) with  $\nu = 0$ , we have

$$T_{f,i}^{\epsilon(t)} = E_f \epsilon_{f,i} = E_f \epsilon_y^{(t)} \cos^2 \alpha_{f,i}.$$

At each step we recalculate  $T_{f,i}$  according to

$$T_{f,i}^{(t+1)} = \begin{cases} T_{f,i}^{\epsilon(t+1)} + T_{f,i}^{r(t)} + \frac{\sum_{j=1}^{n_b} \cos \alpha_{f,b(j)} X_{b(j)}}{(n - N_b) \cos \alpha_{f,i}}, & \text{for } T_{f,i}^{(t+1)} < X_i, \\ 0, & \text{otherwise,} \end{cases} \tag{11}$$

where  $b(j)$  is the index number of the  $j^{\text{th}}$  failed fiber (that is, the  $j^{\text{th}}$  failed fiber is fiber  $b(j)$  in the yarn),  $n_b$  is the number of new broken fibers when going from step  $t$  to  $t + 1$ , and  $N_b$  is the total number of broken fibers at  $t + 1$ . In this equation, we see a stress enhancement effect in the benefactor fiber (along its axis) that results when it has a larger helix angle compared to the fiber that failed.

The TM-ELS rule is embodied in the RHS of Equation (11), which has three terms: the first term is the stress carried by the fiber as if all the fibers are intact, the sum of the first and second terms is the stress in (i) on page 1432, the numerator of the third term comes from (ii) and (iii), and the denominator in the third term accounts for (iv). We note that  $t$  does not necessarily correspond to an increment in the applied loading; the index  $t$  is increased either

- (a) when we increase the external load level, or
- (b) when at a given external load level, the redistribution of stresses leads to failure of more fibers.

**4.4. Bundle stress.** The cross-sectional area of the bundle (neglecting void space between fibers) is given by

$$\bar{A} = \sum_{k=1}^l \frac{n_k A}{\cos \alpha_k} = \sum_{i=1}^n \frac{A}{\cos \alpha_{f,i}}, \tag{12}$$

where  $A$  is the fiber cross-sectional area perpendicular to the fiber axis. The nominal bundle stress  $\sigma$  is the sum of the fiber force components resolved along the bundle axis divided by the bundle area  $\bar{A}$

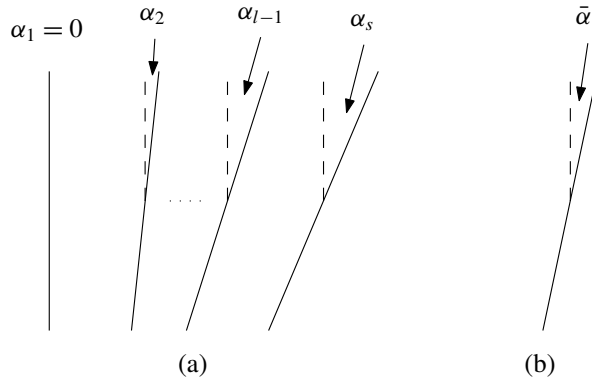


**Figure 4.** Simplified yarn geometry. (a) Layer configuration with multiple angles, (b) simplified geometry where all layers have the same helix angle,  $\bar{\alpha} = \cos^{-1}(\sum_{k=1}^l n_k \cos(\alpha_k)/n)$ , which is the mean helix angle in the general case. The dashed lines indicate the yarn axis direction.

[Phoenix 1979]

$$\sigma = \frac{\sum_{i=1}^n T_{f,i} A \cos \alpha_{f,i}}{\bar{A}} \tag{13}$$

Substituting Equation (12) into Equation (13), we have

$$\sigma = \frac{\sum_{i=1}^n T_{f,i} \cos \alpha_{f,i}}{\sum_{k=1}^l \frac{n_k}{\cos \alpha_k}} = \frac{\sum_{i=1}^n T_{f,i} \cos \alpha_{f,i}}{\sum_{i=1}^n \frac{1}{\cos \alpha_{f,i}}} \tag{14}$$

Note that the stresses in individual surviving fibers will be larger than  $\sigma$  especially when some fibers have failed.

**4.5. Analytical model based on geometrical averaging.** In this section, we develop a probabilistic bundle strength model that averages the fiber helical paths across the bundle to obtain a uniform bundle geometry. In doing so, we define a mean helix angle,  $\bar{\alpha}$ , for the ideal helical structure given as

$$\bar{\alpha} = \cos^{-1} \left( \frac{\sum_{k=1}^l n_k \cos \alpha_k}{n} \right), \tag{15}$$

so that  $\bar{\alpha}$  is weighted by the fraction of all the fibers in each layer  $n_k/n$ , which increases when traveling from center to the surface of the bundle. In essence, this model considers all the fibers to follow the same helical path with  $\bar{\alpha}$  then the TM-ELS rule of Equation (11) reduces to

$$T_{f,i}^{(t+1)} = \begin{cases} T_{f,i}^{\epsilon(t+1)} + T_{f,i}^{r(t)} + \frac{\sum_{j=1}^{n_b} X_{b(j)}}{(n-N_b)}, & \text{for } T_{f,i}^{(t+1)} < X_i, \\ 0, & \text{otherwise,} \end{cases} \tag{16}$$

$$T_{f,i}^{(0)} = T^{(0)} = E_{f\epsilon_y}^{(0)} \cos^2 \bar{\alpha}, \tag{17}$$

where the second line gives the initial stress at  $t = 0$  and where  $\epsilon_y^{(0)}$  is the initially applied bundle strain.

Combining Equations (16) and (17) shows that all intact fibers will sustain the same stress along the fiber axis, that is,

$$T_{f,i}^{(t+1)} = \begin{cases} T & \text{for } T_{f,i}^{(t+1)} < X_i, \\ 0 & \text{otherwise.} \end{cases} \tag{18}$$

In Equation (14), replacing  $\cos \alpha_{f,i}$  by  $\cos \bar{\alpha}$  given in Equation (15), the nominal bundle stress along the bundle axis becomes

$$\sigma = \frac{\sum_{i=1}^n T_{f,i} \cos^2 \bar{\alpha}}{n},$$

and by Equation (18), when there are  $N_b$  failed fibers,  $\sigma$  becomes

$$\sigma = \left(\frac{n - N_b}{n}\right) T \cos^2 \bar{\alpha}. \tag{19}$$

The instantaneous fiber stress component acting along the bundle axis is  $s = T \cos^2 \bar{\alpha}$ , whereby Equation (19) simplifies to

$$s = \left(\frac{n}{n - N_b}\right) \sigma,$$

which is the well-known ELS expression for  $s$  as a function of  $\sigma$ ,  $n$ , and  $N_b$ .

The idea of a mean angle  $\bar{\alpha}$  and an equivalent stress  $T$  for all fibers may well represent the condition of complete migration, which occurs over a short yarn length scale. In this case, a fiber resides in a particular layer only over a very short distance along the yarn axis. Thus, its local tension at a particular cross section is more reflective of the average helix angle than the helix angle of the layer in which it currently resides.

For Weibull fibers under stress  $T$  along its axis, the corresponding fiber failure cumulative probability distribution function (cdf)  $F(T)$  is

$$F(T) = 1 - \exp \left\{ -\left(\frac{T}{\sigma_\delta}\right)^\rho \right\}. \tag{20}$$

As in Daniels' bundle theory, we cast  $F(T)$  in terms of  $s$ , the fiber stress acting along the bundle axis. Substituting  $s = T \cos^2 \bar{\alpha}$  into Equation (20) yields

$$F(s) = 1 - \exp \left\{ -\left(\frac{s}{\cos^2 \bar{\alpha} \sigma_\delta}\right)^\rho \right\}.$$

Following geometric averaging, the strength of a twisted bundle corresponds to that for a parallel bundle of fibers whose strengths follow a Weibull distribution with the same shape parameter  $\rho$  but a 'modified' scale parameter  $\sigma_{\delta,\alpha} = \cos^2 \bar{\alpha} \sigma_\delta$ . Hence, the asymptotic distribution function for bundle strength will be Gaussian with mean  $\mu_G$  and standard deviation  $\gamma_G$  given by

$$\mu_G = \sigma_{\delta,\alpha} (\rho e)^{-1/\rho} = \mu_D \cos^2 \bar{\alpha}, \quad \gamma_G = \left(\frac{\sigma_{\delta,\alpha}}{\sqrt{n}}\right) \rho^{-1/\rho} \sqrt{e^{-1/\rho} (1 - e^{-1/\rho})} = \gamma_D \cos^2 \bar{\alpha},$$

where  $\mu_D$  and  $\gamma_D$  are the mean strength and standard deviation of a Daniels parallel fiber bundle given by Equation (5).

Using the [Smith 1982; McCartney and Smith 1983] corrections we obtain improved estimates,  $\mu_G^*$  and  $\gamma_G^*$ , for the mean and standard deviation:

$$\mu_G^* = \mu_D \cos^2 \bar{\alpha} \left\{ 1 + \frac{0.996}{n^{2/3}} \left( \frac{e^{2/\rho}}{\rho} \right)^{1/3} \right\}, \quad \gamma_G^* = \gamma_D \cos^2 \bar{\alpha} \sqrt{1 - 0.317 \left( \frac{\mu_D}{\gamma_D} \right)^2 \left( \frac{e^{2/\rho}}{n^2 \rho} \right)^{2/3}}.$$

**4.6. Analytical model based on statistical averaging.** In this section, we develop a second probability model for bundle strength, based on statistical averaging, where we average the failure probabilities of the fibers across the layers in an ideal helical structure. In doing so, we find it convenient to change to a continuous description of the bundle geometry. We let  $\bar{r} = r/R$ , that is, the radial distance normalized by yarn radius, so that  $\bar{r} = 0$  is the yarn axis and  $\bar{r} = 1$  corresponds to the yarn radius. The fiber helix angle  $\alpha(\bar{r})$  is taken as a continuous function of  $\bar{r}$ . Accordingly,  $\alpha(\bar{r} = 0) = 0$  and  $\alpha(\bar{r} = 1) = \alpha_s$ . Likewise we let  $n_r(\bar{r})$  be the number of fibers within a cylinder of radius  $\bar{r}$ , taking it to be a continuous function of  $\bar{r}$ . Thus  $n_r(\bar{r} = 0) = 0$  and  $n_r(\bar{r} = 1) = n$ . Therefore  $dn_r(\bar{r})/n$  is the fraction of fibers between  $\bar{r}$  and  $\bar{r} + d\bar{r}$ .

As mentioned earlier, the fiber stresses  $T_{f,i}$  are generally a sum of the stress generated from the applied loading, assuming no fiber breaks,  $T_{f,i}^\epsilon$ , and the stress components transferred from broken fibers,  $T_{f,i}^r$ . The former stresses are distributed nonuniformly depending on the fiber helix angles, whereas the latter additional stresses transferred from fiber breaks will resolve to have same components acting along the yarn axis according to the TM-ELS rule described above. As fiber failures accumulate, these latter contributions,  $T_{f,i}^r$ , typically greatly exceed the nonuniform contributions  $T_{f,i}^\epsilon$ . In this case, the component of  $T_{f,i}$  acting along the yarn axis can be reasonably considered equal for all fibers, and thus, taken as  $s = T_{f,i} \cos^2 \alpha(\bar{r})$ , as defined earlier. Accordingly, the probability of failure  $F(T_{f,i})$  for fiber  $i$ , with helix angle  $\alpha(\bar{r})$ , in terms of  $s$  is

$$F(s) = 1 - \exp \left\{ - \left( \frac{s}{\sigma_\delta \cos^2 \alpha(\bar{r})} \right)^\rho \right\}.$$

The assumption that the component of stress along the yarn axis,  $s$ , is equal for all fibers greatly simplifies the calculation of average failure probability across the yarn cross-section. Denoting this average as  $\bar{F}(s)$ , we have

$$\bar{F}(s) = \int_{\alpha=0}^{\alpha_s} \left[ 1 - \exp \left\{ - \left( \frac{s}{\sigma_\delta \cos^2 \alpha(\bar{r})} \right)^\rho \right\} \right] \frac{dn_r(\bar{r})}{n}. \tag{21}$$

The functions  $n_r(\bar{r})$  and  $\alpha(\bar{r})$  are calculated from the bundle packing density  $\nu(\bar{r})$ . As in [Phoenix 1979], for large bundles we take

$$\nu(\bar{r}) = \frac{\phi^{(\infty)}}{\pi} \cos \alpha(\bar{r}), \quad \phi^{(\infty)} = \frac{1}{2}(1 + \sec \alpha_s), \tag{22}$$

for  $0 \leq \bar{r} \leq 1$ . Equation (22) assumes that the fiber packing density is uniform in the yarn cross-section, that is, the void fraction is constant with respect to radial position. (Actually, the void fraction may be expected to decrease slightly as  $r$  decreases, since the radial pressure in the yarn increases from yarn surface to the yarn center. Nevertheless, such effects are difficult to model, and little is believed to be lost with the uniform packing assumption.) Since  $\nu(\bar{r})$  satisfies

$$\int_0^1 \nu(\bar{r}) 2\pi \bar{r} d\bar{r} = 1,$$

the fraction of all fibers within a cylinder of radius  $\bar{r}$  can be written as

$$\frac{n_r(\bar{r})}{n} = \int_0^{\bar{r}} v(\bar{r}) 2\pi \bar{r} d\bar{r}.$$

Upon differentiating this equation with respect to  $\bar{r}$ , we get

$$\frac{dn_r(\bar{r})}{n} = \frac{\phi^{(\infty)}}{\pi} \cos \alpha(\bar{r}) 2\pi \bar{r} d\bar{r}. \tag{23}$$

Substituting Equation (23) into Equation (21), the ‘average’ probability distribution for fiber failure can be rewritten in terms of  $\alpha(\bar{r})$  only as

$$\bar{F}(s) = \int_{\alpha=0}^{\alpha_s} \left[ 1 - \exp \left\{ - \left( \frac{s \sec^2 \alpha(\bar{r})}{\sigma_\delta} \right)^\rho \right\} \right] \frac{\phi^{(\infty)}}{\pi} \cos \alpha(\bar{r}) 2\pi \bar{r} d\bar{r}. \tag{24}$$

For an ideal yarn geometry we have

$$\tan \alpha(\bar{r}) = \frac{2\pi \bar{r}}{\bar{h}}, \tag{25}$$

where  $\bar{h} = h/R$  and at the surface of the yarn

$$\tan \alpha_s = \frac{2\pi}{\bar{h}}. \tag{26}$$

From Equation (25) we get

$$\sec^2 \alpha d\alpha = \frac{2\pi}{\bar{h}} d\bar{r}. \tag{27}$$

Substituting Equations (24)–(27) into Equation (21) yields

$$\begin{aligned} \bar{F}(s) &= \frac{2\phi^{(\infty)}}{\tan^2 \alpha_s} \int_{\alpha=0}^{\alpha_s} \left[ 1 - \exp \left\{ - \left( \frac{s \sec^2 \alpha}{\sigma_\delta} \right)^\rho \right\} \right] \tan \alpha \sec \alpha d\alpha \\ &= 1 - \frac{2\phi^{(\infty)}}{\tan^2 \alpha_s} \int_{\alpha=0}^{\alpha_s} \exp \left\{ - \left( \frac{s \sec^2 \alpha}{\sigma_\delta} \right)^\rho \right\} \tan \alpha \sec \alpha d\alpha \\ &= 1 - \frac{2\phi^{(\infty)}}{\tan^2 \alpha_s} \int_1^{\sec \alpha_s} \exp \left\{ - \left( \frac{s}{\sigma_\delta} \right)^\rho x^{2\rho} \right\} dx \\ &= 1 - \frac{\phi^{(\infty)}}{\rho \tan^2 \alpha_s} \left( \frac{s}{\sigma_\delta} \right)^{-1/2} \int_{(s/\sigma_\delta)^\rho}^{(s/\sigma_\delta)^\rho \sec^{2\rho} \alpha_s} e^{-y} y^{1/2\rho-1} dy, \end{aligned} \tag{28}$$

where in the third line we made the change of variables  $\sec \alpha = x$ , and again in the fourth line as  $y = (s/\sigma_\delta)^\rho x^{2\rho}$ . The integral in Equation (28) can be written in terms of upper incomplete Gamma functions [Abramowitz and Stegun 1964] as shown below

$$\bar{F}(s) = 1 - \frac{\phi^{(\infty)}}{\rho \tan^2 \alpha_s} \left( \frac{s}{\sigma_\delta} \right)^{-1/2} \left[ \Gamma \left( \frac{1}{2\rho}, \left\{ \frac{s}{\sigma_\delta} \right\}^\rho \right) - \Gamma \left( \frac{1}{2\rho}, \left\{ \frac{s}{\sigma_\delta} \right\}^\rho \sec^2 \alpha_s \right) \right].$$

In statistical averaging, the problem for a twisted bundle reduces to that for a parallel fiber bundle with fiber strength probability distribution given by  $\bar{F}(s)$ . As a result, the bundle strength is asymptotically

normal where the asymptotic bundle mean strength and standard deviation are given by

$$\mu_S = s^*[1 - \bar{F}(s^*)], \quad \gamma_S = \frac{s^*}{\sqrt{n}} \sqrt{\bar{F}(s^*)[1 - \bar{F}(s^*)]},$$

where  $s^*$  is the point where the maximum of  $\mu(s)$  occurs. The final result according to statistical averaging is calculated by applying corrections due to [Smith 1982; McCartney and Smith 1983]. Thus, the improved estimates for the mean and standard deviation,  $\mu_S^*$  and  $\gamma_S^*$  are

$$\mu_S^* = \mu_S + \bar{\Delta}_n^*, \quad \gamma_S^* = \gamma_S \sqrt{1 - 0.320 \left(\frac{\bar{\Delta}_n^*}{\gamma_S}\right)^2},$$

where

$$\bar{\Delta}_n^* = \frac{0.996}{n^{2/3}} \left\{ \frac{\bar{F}'(s^*)^2 s^{*4}}{2\bar{F}'(s^*) + s^* \bar{F}''(s^*)} \right\}^{1/3}.$$

### 5. Simulation algorithms

We now discuss the Monte Carlo simulation algorithm for the failure of a twisted bundle of Weibull fibers having shape parameter  $\rho$ , and scale parameter  $\sigma_\delta$ . These fibers are assumed to have identical diameter, cross-sectional area, and Young’s modulus, and are arranged in  $l$  layers having ideal helical structure. For a given twisted bundle surface helix angle,  $\alpha_s$ , the helix angle of each layer can be determined using Equation (9). The number of fibers in each layer,  $n_k$ , can be determined using Equation (8) and the total number of fibers  $n$  is the sum.

For a given set of values of the above parameters, we first assign a Weibull strength to each of the  $n$  fibers. We assume that these fibers are twisted without tension so the fibers do not have any pre-stress or pre-strain. For a given set of parameter values, the number of replications performed by the Monte Carlo simulation is  $n_s$ .

Starting from zero, we can either apply a monotonically increasing uniform stress or strain. Both algorithms are described briefly below. These two algorithms yield the same empirical probability distribution and mean strength results except that the stress-strain curves obtained by these two algorithms exhibit different characteristics. In a stress-controlled experiment failure is sudden and the external load drops from the maximum to zero. In a strain-controlled experiment, the bundle stress starts from zero, attains a maximum defined as the strength, and then decreases to zero while the bundle strain is monotonically increased indefinitely.

**5.1. Stress-controlled experiment.** In a stress-controlled experiment the stress is increased incrementally in predetermined small steps. Whenever a step encounters a fiber for which its axial stress exceed its strength, the fiber is broken and then its stress is distributed equally among the intact fibers according to TM-ELS. The algorithm then checks to see if the additional loads on the survivors would result in any of their assigned strengths being exceeded, and if so, these fibers are then broken and their updated loads are redistributed. If not, equilibrium has been achieved at that step in which case new incremental steps in external load are applied until some survivors have their strengths exceeded. These fibers are then broken and the stress redistribution process is repeated.

Eventually we reach bundle collapse whereby all remaining fibers fail with no further increase in the applied stress. The threshold external stress beyond which all the fibers fail is recorded as the bundle strength.

**5.2. Strain-controlled experiment.** In a strain-controlled experiment we do not have to explicitly redistribute the load from broken fibers to intact ones. At each increment in applied bundle strain we calculate fiber strains for each layer. If the strain of a fiber in some layer exceeds its failure strain then that fiber becomes broken and the external bundle load and stress for that bundle strain is recalculated. The bundle stress at increment number  $t$  is then given by

$$\sigma^{(t)} = \frac{\sum_{i=1}^n E_t \epsilon_{f,i}^{(t)} \cos \alpha_{f,i}}{\sum_{i=1}^n \frac{1}{\cos \alpha_{f,i}}}, \quad \epsilon_{f,i}^{(t)} = \begin{cases} \epsilon_{f,i} & \text{for } \epsilon_{f,i} < \xi_i, \\ 0 & \text{otherwise,} \end{cases}$$

where  $\xi_i$  is the failure strain of fiber  $i$ . The bundle strength is given by  $\text{strength} = \max_t \{\sigma^{(t)}\}$ .

## 6. Results and discussion

In this section, we discuss and compare the theoretical and Monte Carlo simulation results for the strength of a twisted fiber bundle.

**6.1. Validation of simulation algorithm.** As a form of validation we performed Monte Carlo simulation for the case of a parallel fiber bundle, that is,  $\alpha_s = 0$ . In Figure 5 the simulated bundle mean strength and asymptotic standard deviation normalized by  $\sigma_\delta$  are compared with corrected Daniels' values,  $\mu_D^*$  and  $\gamma_D^*$ , normalized by  $\sigma_\delta$ , given by Equation (7), as  $\rho$  varies from 2 to 10. Note that all estimates for the mean and standard deviation in Figure 5 are normalized by  $\sigma_\delta$ . We achieve good agreement between the parallel bundle theory and simulation for the entire range of  $\rho$  and both bundle sizes considered,  $n = 130$  and  $n = 1185$ . If corrections by [Smith 1982; McCartney and Smith 1983] are not applied, then  $\mu_D$  slightly underestimates and  $\gamma_D$  overestimates the corresponding simulated values. The means for different bundle sizes differ only slightly because of the correction to the Daniels' value. Likewise the standard deviation values will collapse almost onto one curve when scaled by  $\sqrt{n}$  (not shown in the figure).

**6.2. Failure behavior.** From the simulation results we have noticed that both  $\alpha_s$  and  $\rho$  clearly affect the nature of failure. In the case of low  $\alpha_s$  and low  $\rho$  the fiber breaks are spread randomly across the cross-section of the bundle. Also the fraction of failed fibers when the maximum bundle stress is achieved is relatively high, indicative of a ductile-type failure process. In the case of high  $\alpha_s$  and high  $\rho$  there are relatively fewer failed fibers when the peak bundle stress is reached, and these are more likely to concentrate near the center of the bundle, indicative of a brittle-type failure.

The observed transitions in failure mode are a consequence of the interaction of  $\rho$  and the strain distribution among the layers, which depends on  $\alpha_s$ . As the variation in fiber strength increases ( $\rho$  decreases) failure progression becomes dominated by the widely dispersed fiber strengths. It is more dispersed for lower  $\alpha_s$ , as the variation in fiber strains across the bundle is mild. As the variation in fiber strength decreases ( $\rho$  increases) failure progression becomes dominated by the fiber strain distribution. In this case, as we increase  $\alpha_s$  the gradient in strain between the highly strained center and less strained surface layers steepens, promoting failure to be localized towards the center.

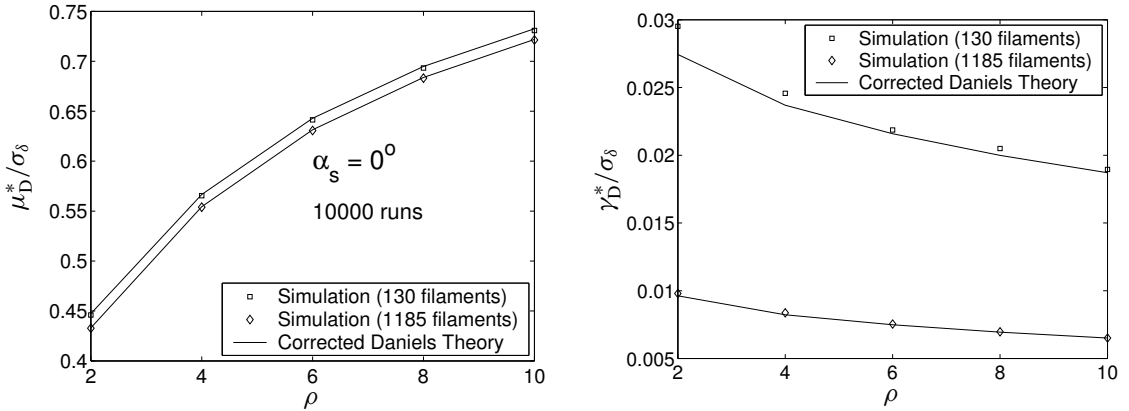


**Figure 5.** Normalized mean and asymptotic standard deviation for bundle strength obtained from Monte Carlo simulation ( $n_s = 10000$ ) as compared with the corresponding corrected Daniels' values given by Equation (7).

**6.3. Stress-strain curves.** Figure 6 shows average stress-strain curves (average of 500 runs) for bundles with 62 and 1185 fibers, respectively, but otherwise the same parameter values  $\alpha_s = 12^\circ$ ,  $\rho = 2$  and 8. Also shown are sample stress-strain curves for three successive realizations. For the smaller bundle with only 62 fibers the sample stress-strain curves show significant deviation from the average behavior reaching 5-10% near the peak stress. This implies that for a long chain of such bundles one might expect the chain to be much weaker than the average bundle strength as the strength would be governed by the weakest bundle. On the other hand, for the 1185 fiber bundle the deviations are much smaller being 1-2%, so a long chain of such bundles would be much closer to the average bundle strength. The fluctuations in the bundle strength grow as the variation in fiber strength increases, such as when  $\rho = 8$  decreases to  $\rho = 2$ .

Figure 6 shows that the initial bundle modulus is independent of  $\rho$ . This high initial modulus occurs because of the initiation of a relatively few randomly dispersed breaks. After further straining, the slope of the stress-strain curve decreases at a rate which depends on  $\rho$ , since this controls the variability and thus, the rate at which weak fibers are encountered as strain increases. Eventually the peak stress is reached when loss of fibers through breakage outweighs the increased stresses occurring in the survivors with increasing strain, these being different from fiber to fiber. (In the stress-controlled experiment this corresponds to the stress (and strain) at which instability is reached and sudden collapse occurs.) Concomitantly the stress drops with further straining at a rate which also depends on  $\rho$ , becoming more abrupt and brittle-like as  $\rho$  increases.

**6.4. Cumulative probability density functions.** Figure 7 shows the simulated cumulative probability distribution function for the strength of a twisted fiber bundle on normal probability paper, namely,  $\text{erf}^{-1}(2G_n - 1)$  vs.  $S/\sigma_\delta$ , where we recall that  $G_n$  is the bundle strength cumulative distribution function. The linearity of the distributions suggests that in all cases the strength distribution is virtually normal. Figure 7a displays its dependence on the surface helix angle  $\alpha_s$ , ( $\alpha_s = 0^\circ, 6^\circ, 12^\circ, 18^\circ, 24^\circ$ )

for the case of  $\rho = 6$  and  $n = 1185$ . Figure 7b shows its dependence on bundle size  $n$ , ( $n = 130, 653, 1185$ ) for  $\rho = 4$  and  $\alpha_s = 12^\circ$ . From Figure 7a we find that the strengths decrease substantially as  $\alpha_s$  increases, while the standard deviation (inversely related to the slope of the curves) stays more or less independent of  $\alpha_s$  and Figure 7b shows that the bundle size  $n$  has its most significant impact on the bundle standard deviation, which is approximately inversely proportional to  $n$ . Also shown in Figure 7 are the corresponding predictions from the model based on statistical averaging. In general, we find that when  $\alpha_s < 18^\circ$  the model achieves very good agreement with the simulation result. For larger values of  $\alpha_s$ , the model provides a conservative estimate.

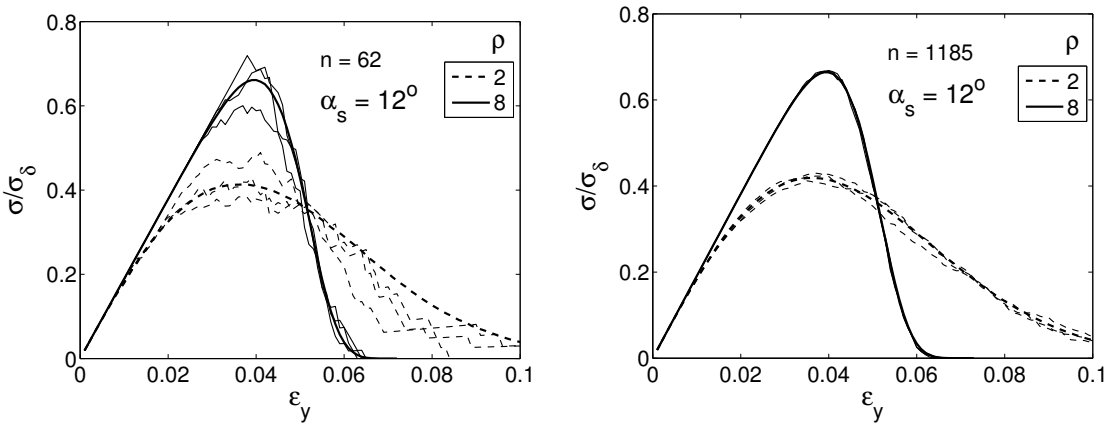


**Figure 6.** Thin lines are sample stress strain curves and thick lines are average (of 500 runs) stress strain curves for given values of  $\rho$ ,  $\alpha_s$ , and  $n$ .

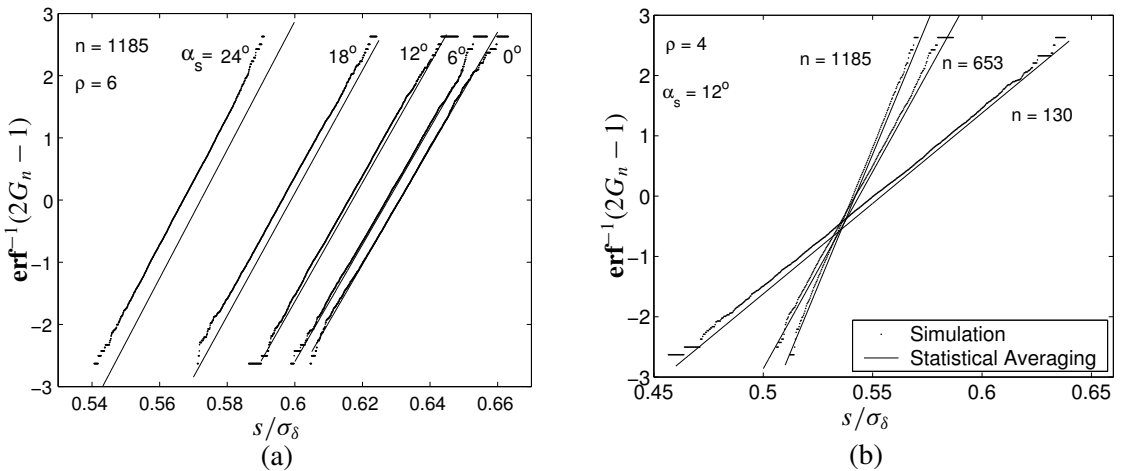


**Figure 7.** Distribution functions on normal probability paper ( $\text{erf}^{-1}(2G_n - 1)$  versus  $S/\sigma_\delta$ ) for 10000 replications. The parameters used for these plots are (a)  $n = 1185$ ,  $\rho = 6$  and  $\alpha_s = 0^\circ, 6^\circ, 12^\circ, 18^\circ, 24^\circ$ ; (b)  $\rho = 4$ ,  $\alpha_s = 12^\circ$  and  $n = 130, 653, \text{ and } 1185$ . Here  $S$  is the strength of the bundle obtained either from the simulation or size corrected statistical averaging theory.

**6.5. Strength and standard deviation efficiency, and coefficient of variation.** To study the dependence of the mean bundle strength on  $\alpha_s$  and  $\rho$ , we calculate the strength efficiency of the fiber bundle,  $\mathcal{E}_\mu$ , which is the ratio of mean bundle strength to mean fiber strength,

$$\mathcal{E}_\mu = \frac{\mu^*}{E(X)},$$

where  $\mu^*$  is the mean bundle strength for given  $n$  obtained either using one of the theories (corrected for  $n$ ) or a simulation and  $E(X)$  is the mean strength of the fiber. For Weibull fibers,  $E(X) = \sigma_\delta \Gamma(1 + 1/\rho)$ , where  $\Gamma(\cdot)$  is the Gamma function. For instance, in the case of geometrical averaging, the strength efficiency for a very large bundle (not requiring a size correction) is the closed form expression

$$\mathcal{E}_\mu^{(\infty)} = \frac{\cos^2 \bar{\alpha} \sigma_\delta (\rho e)^{-1/\rho}}{\sigma_\delta \Gamma(1 + 1/\rho)} = \frac{\cos^2 \bar{\alpha} (\rho e)^{-1/\rho}}{\Gamma(1 + 1/\rho)},$$

which depends only on the mean helix angle,  $\bar{\alpha}$ , and Weibull shape parameter,  $\rho$ .

Another useful quantity for reflecting variability in the bundle strength is the coefficient of variation, ( $\mathcal{CV}$ ), which is the ratio of the standard deviation to the mean, expressed as

$$\mathcal{CV} = \frac{\gamma^*}{\mu^*}. \quad (29)$$

For a measure of the statistical variation in bundle strength compared to that of a single fiber, we define the transfer efficiency of the variability as the ratio of the bundle standard deviation to the fiber standard deviation, that is

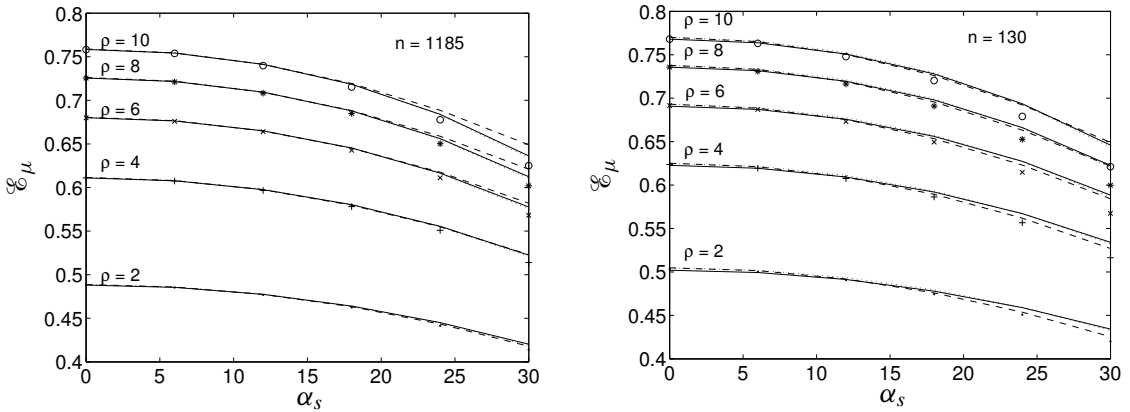
$$\mathcal{E}_\gamma = \frac{\gamma^*}{\sqrt{\text{Var}(X)}}, \quad (30)$$

where  $\text{Var}(X)$  is the variance of fiber strength  $X$ . Again the bundle  $\gamma^*$  and  $\mu^*$  are calculated for a given  $n$  either from one of the three theories (corrected for  $n$ ) or simulation. In the case of geometrical averaging, Equations (29) and (30) for a large bundle (not requiring a size correction) become

$$\mathcal{CV}^{(\infty)} = \sqrt{\frac{1 - e^{-1/\rho}}{n e^{-1/\rho}}}, \quad \mathcal{E}_\gamma^{(\infty)} = \frac{\cos^2 \bar{\alpha} \rho^{-1/\rho} \sqrt{e^{-1/\rho} (1 - e^{-1/\rho})}}{\sqrt{n [\Gamma(1 + 2/\rho) - \Gamma^2(1 + 1/\rho)]}}.$$

In all theories  $\mathcal{CV}$ ,  $\mathcal{E}_\mu$ , and  $\mathcal{E}_\gamma$  are independent of  $\sigma_\delta$ .

Figure 8 compares simulation and theoretical predictions for  $\mathcal{E}_\mu$  vs.  $\alpha_s$  for different values of  $\rho$ . Generally  $\mathcal{E}_\mu$  decreases as  $\rho$  decreases (that is, the variability in the fiber strength increases) and  $\alpha_s$  increases. As  $\alpha_s$  increases, more fibers in the bundle become misaligned with the direction of loading. As  $\rho$  decreases, a higher proportion of weaker fibers exists in the bundle. Figure 8 shows that all theories capture the effects of  $\rho$  and  $\alpha_s$  on the strength efficiency of the twisted fiber bundle very well. For both  $n = 130$  and 1185 and smaller  $\alpha_s$  (up to  $18^\circ$ ) there is almost no difference between theory and simulation. However, for higher values of  $\alpha_s$  there are slight differences, which diminish as  $\rho$  decreases, that is, the variability increases and a rather diffuse-type of failure mode occurs. TM-ELS translates to a diffuse failure pattern when  $\alpha_s$  and  $\rho$  are low, but not when they are both high. Therefore the discrepancy between theory and simulation at high  $\rho$  and high  $\alpha_s$  is attributed to the fact that under these conditions the failure is more or less localized near the center of the yarn, up to the point of collapse.



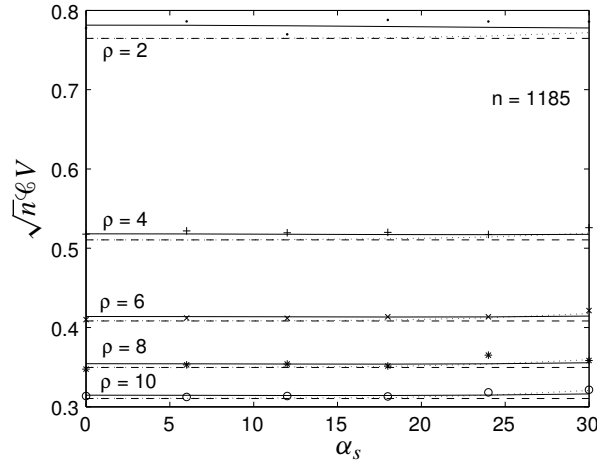
**Figure 8.** Strength efficiency,  $\mathcal{E}_\mu$ , versus surface helix angle,  $\alpha_s$ . Dashed and solid lines correspond to theories based on geometrical averaging and statistical averaging, respectively. Dotted lines are obtained using the theory of [Phoenix 1979]. The marker points are simulation results.

Figure 9 depicts the behavior of the  $\mathcal{C}^V$  for  $n = 1185$ . The simulation results show that it is independent of  $\alpha_s$  with the exception of a slight drop in  $\mathcal{C}^V$  at a high value of  $\alpha_s$  ( $\approx 25^\circ$ ). The latter drop can again be attributed to less variability in the failure patterns from one bundle to another, as  $\alpha_s$  increases. The agreement between the theories and simulation is very good. In cases of smaller  $\rho$ , the statistical averaging model performs better than the other theories discussed earlier. For smaller bundles,  $n = 130$  and lower  $\rho < 4$  the discrepancies between the asymptotic theories and simulation increase as shown in Figure 10. The thick lines in Figure 10 are the  $\mathcal{C}^V$  predictions with corrections applied to both the mean and standard deviation, that is,  $\mathcal{C}^V = \mu^*/\gamma^*$ , as in Figure 9. Again in these cases, the statistical averaging model outperforms the others. The thinner lines in Figure 10 correspond to the  $\mathcal{C}^V$  calculations when correcting the mean only,  $\mathcal{C}^V = \mu^*/\gamma$ , which is shown to provide a conservative estimate.

Figure 11 shows the dependence of  $\mathcal{E}_\gamma$  on  $\rho$  and  $\alpha_s$ . While  $\gamma$  and the  $\mathcal{C}^V$  increase as the variability in fiber strength increases ( $\rho$  decreases), the  $\mathcal{E}_\gamma$  decreases (improves). As shown, the theories provide equally good agreement for  $n = 1185$ , but for  $n = 130$ , the statistical averaging model consistently provides values closer to the simulation results. Also, given in Table 1 are dimensional values of bundle strength mean and standard deviation to show how they compare.

### 7. Effect of friction and chain-of-bundles calculation

Beginning with the model for the failure of a single bundle as introduced earlier in the paper, we outline a basic framework for predicting the strength of a twisted yarn of length  $L$ . For this, we apply the chain-of-bundles (COB) model, where the strength of weakest bundle in the chain is the strength of the chain. The COB model requires defining the length of each bundle or link in the chain, that is, a “characteristic stress transfer length”, which is appropriately defined by the fiber length needed for the fiber to recover the stress away from a break. This length depends on the interfiber friction as well as the contact pressures



**Figure 9.** Coefficient of variation scaled with bundle size,  $\sqrt{n}CV$ , vs surface helix angle,  $\alpha_s$  for  $n = 1185$ , and  $\rho = 2, 4, 6, 8,$  and  $10$ . Dashed and solid lines correspond to theories based on geometrical averaging and statistical averaging, respectively. Dotted lines are obtained using the theory of [Phoenix 1979]. The marker points are simulation results.

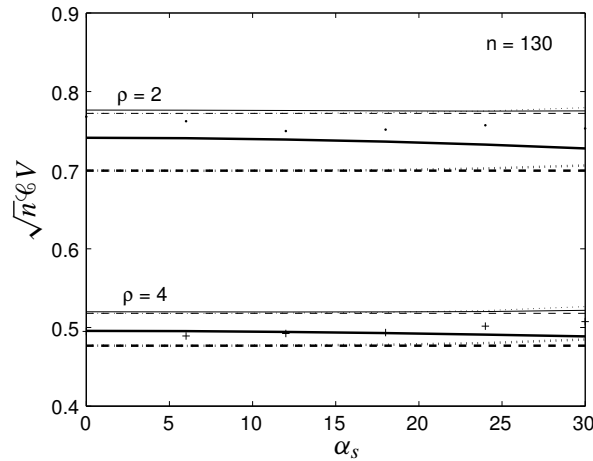


**Figure 10.** Coefficient of variation scaled with bundle size,  $\sqrt{n}CV$ , vs surface helix angle,  $\alpha_s$ . Thick lines correspond to values where correction to both strength mean and standard deviation are applied, and in the case of thin lines, correction is applied to strength mean only. Dashed and solid lines correspond to theories based on geometrical averaging and statistical averaging, respectively. Dotted lines are obtained using the theory of [Phoenix 1979]. The marker points are simulation results.

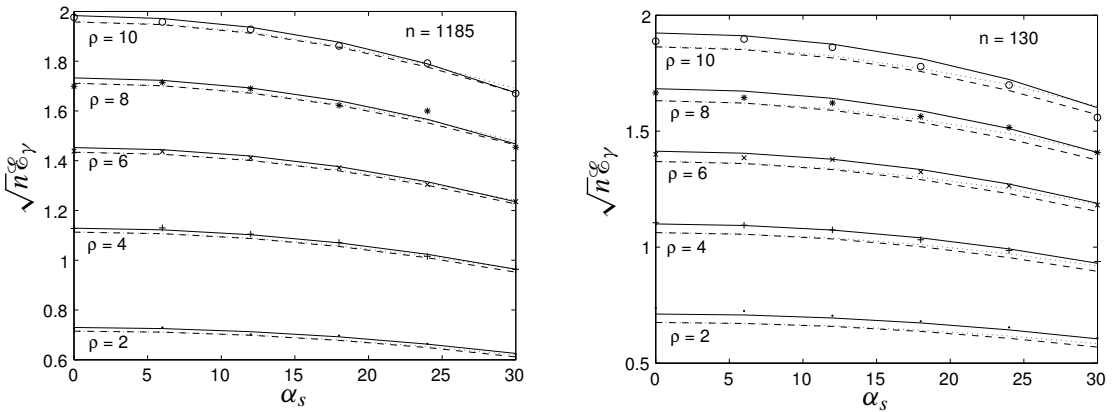


**Figure 11.** Transfer efficiency of the variability  $\sqrt{n\epsilon_\gamma}$  versus surface helix angle  $\alpha_s$ . The left one is for 1185 fibers and the right one is for 130 fibers. Dashed and solid lines correspond to theories based on geometrical averaging and statistical averaging, respectively. Dotted lines are obtained using the theory of [Phoenix 1979]. The marker points are simulation results.

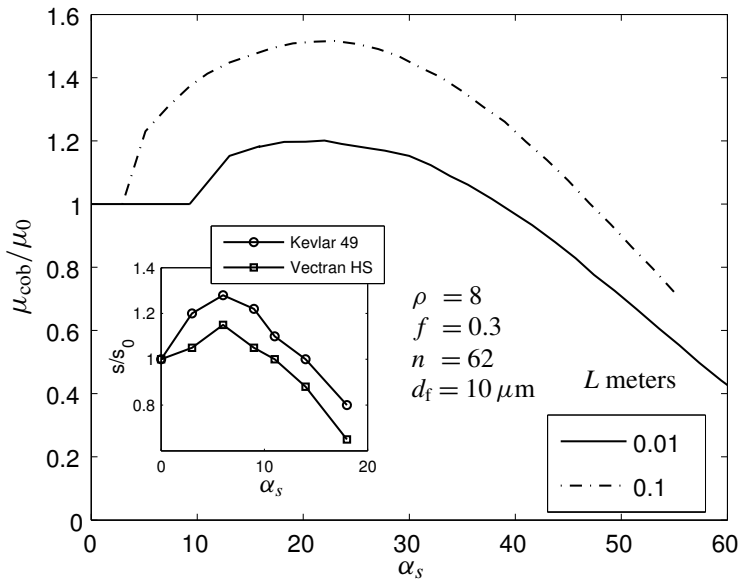


**Figure 12.** Normalized mean yarn strength versus surface helix angle  $\alpha_s$  for yarn length  $L$ . Here  $\mu_0$  is the strength of the yarn when  $\delta_c = L$ . Inset figure (normalized yarn strength  $S/S_0$  versus  $\alpha_s$ ) is plotted using data from [Rao and Farris 2000], where  $S_0$  is the yarn strength when  $\alpha_s = 0$ .

between the fibers caused by twisting. A rigorous analysis of friction effects and their impact on this characteristic link length are beyond the scope of this work and are treated in a sequel.

For a simple demonstration of the COB model, we employ a friction length given by [Alexander 1952]

$$l_f = \frac{\beta_A d_f}{(1 - \phi_A) f \sin^2 \alpha_A},$$

where  $f$  is the friction coefficient,  $\phi_A$  and  $\beta_A$  are two adjustable parameters, taken by Alexander to be  $1/2$ , and  $\alpha_A$  is the corresponding helix angle satisfying  $\tan \alpha_A = \beta_A \tan \alpha_s$ . We define the characteristic length of a bundle in terms of the friction length, with  $\phi_A = \beta_A = 1/2$ , as

$$\delta_c = 2l_f \cos \alpha_A = \frac{2 d_f \cos \alpha_A}{f \sin^2 \alpha_A} = \delta_c(\alpha_s) = \frac{4d_f \sqrt{4 + \tan^2 \alpha_s}}{f \tan^2 \alpha_s}, \quad (31)$$

where we have rewritten it in terms of  $\alpha_s$ . According to Equation (31), the characteristic length decreases as  $\alpha_s$  increases. The number of bundles in the yarn of length  $L$  is  $m(\alpha_s) = L/\delta_c(\alpha_s)$ , and this number increases with  $\alpha_s$ .

Figure 12 clearly shows that the strength rises, as  $\alpha_s$  increases, up to a maximum around  $30^\circ$ . However, the  $\alpha_s$  corresponding to optimal strength is much higher than what is typically observed, though not very different from what [Alexander 1952] obtained for a staple yarn. In an actual yarn with continuous filaments twisting introduces fiber slack in inner fibers that must be relieved by periodic fiber migration along the yarn. Such migration becomes increasingly difficult as the twist angle increases and thus contact forces increase. For this reason the yarn strength peaks prematurely as slack effects cause uneven fiber load distribution, thus reducing the strength beyond the effect of twist discussed earlier in the paper. On the other hand, in a staple yarn that has discontinuous fibers, these slack effects are easily eliminated by fiber sliding and thus strength peaks at a twist angle much closer to our values. Based on the weakest link concept, it is expected that the strength of the longer yarn with  $L = 0.1$  meters would be smaller than that of the shorter yarn with  $L = 0.01$  meters. Results in Figure 12, which plots normalized mean strength versus surface helix angle, show the reverse because of the much smaller normalization strength  $\mu_0$  for the longer yarn with  $L = 0.1$  meters.

## 8. Conclusions

Monte Carlo simulation and analytical models are developed for the statistical strength of twisted fiber bundles having Weibull fibers. We see important effects like the approximate normality of the bundle

	Strength mean (GPa)	Strength standard deviation (GPa)
Fiber	2.78	0.540
Bundle ( $\alpha_s = 0^\circ$ )	1.88	0.023
Bundle ( $\alpha_s = 30^\circ$ )	1.61	0.020

**Table 1.** Typical bundle strength mean and standard deviation values for a fiber with  $\sigma_\delta = 3$  GPa,  $\rho = 6$ , and  $n = 1185$ .

strength distribution, decrease in strength with number of fibers in bundle, transition from a ductile, for small  $\alpha_s$  and  $\rho$ , to brittle failure mode for large  $\alpha_s$  and  $\rho$ . We further use a simple chain-of-bundles model showing the presence of an optimal twist angle that gives maximum strength. However, a more detailed study, which considers pressure development in the bundle and stress build up in fibers from broken ends, is required to fully understand the effects of friction on bundle strength and optimal  $\alpha_s$ .

## References

- [Abramowitz and Stegun 1964] M. Abramowitz and I. A. Stegun, *Handbook of mathematical functions*, Dover Publications, New York, NY, 1964.
- [Alexander 1952] E. Alexander, “Optimal twist in staple yarn”, *Text. Res. J.* **22**:8 (1952), 503–508.
- [Daniels 1945] H. E. Daniels, “The statistical theory of the strength of bundles of threads I”, *P. Roy. Soc. Lond. A Mat.* **183**:995 (1945), 405–435.
- [Hearle et al. 1969] J. W. S. Hearle, P. Grosberg, and S. Vacker, *Structural mechanics of fibers, yarns, and fabrics*, vol. 1, Wiley-Interscience, 1969.
- [McCartney and Smith 1983] L. N. McCartney and R. L. Smith, “Statistical theory of the strength of fiber bundles”, *J. Appl. Mech. (Trans. ASME)* **50**(3) (1983), 601–608.
- [Naik et al. 2001] N. K. Naik, I. Mudzingwa, and M. N. Singh, “Effect of twisting on tensile failure of impregnated yarns with broken filaments”, *J. Compos. Technol. Res.* **23**:3 (2001), 225–234.
- [Pan 1993] N. Pan, “Prediction of statistical strengths of twisted fibre structures”, *J. Mater. Sci.* **28**:22 (1993), 6107–6114.
- [Phoenix 1979] S. L. Phoenix, “Statistical theory of the strength of twisted fiber bundles with applications to yarns and cables”, *Text. Res. J.* **49**:7 (1979), 407–423.
- [Phoenix and Beyerlein 2000] S. L. Phoenix and I. J. Beyerlein, “Statistical strength theory for fibrous composite materials”, pp. 559–639 in *Comprehensive composite materials*, vol. 1, edited by A. Kelly et al., Pergamon (Elsevier Science), 2000. Chapter 1.19.
- [Rao and Farris 2000] Y. Rao and R. J. Farris, “A modeling and experimental study of the influence of twist on the mechanical properties of high-performance fiber yarns”, *J. Appl. Polym. Sci.* **77**:9 (2000), 1938–1949.
- [Smith 1982] R. L. Smith, “The asymptotic distribution of the strength of a series-parallel system with equal load-sharing”, *Ann. Probab.* **10**:1 (1982), 137–171.
- [Vigolo et al. 2000] B. Vigolo, A. Pénicaud, C. Coulon, C. Sauder, R. Pailler, C. Journet, P. Bernier, and P. Poulin, “Macroscopic fibers and ribbons of oriented carbon nanotubes”, *Science* **290**:5495 (2000), 1331–1334.
- [Zhang et al. 2004] M. Zhang, K. R. Atkinson, and R. H. Baughman, “Multifunctional carbon nanotube yarns by downsizing an ancient technology”, *Science* **306**:5700 (2004), 1358–1361.

Received 11 Dec 2005.

PANKAJ K. PORWAL: [pkp2@cornell.edu](mailto:pkp2@cornell.edu)

Theoretical Division, Los Alamos National Laboratory, Los Alamos, NM 87545, United States  
<http://www.tam.cornell.edu/~pkp2>

IRENE J. BEYERLEIN: [irene@lanl.gov](mailto:irene@lanl.gov)

Theoretical Division, Los Alamos National Laboratory, Los Alamos, NM 87545, United States

S. LEIGH PHOENIX: [slp6@cornell.edu](mailto:slp6@cornell.edu)

Department of Theoretical and Applied Mechanics, Cornell University, Ithaca, NY 14853, United States  
<http://www.tam.cornell.edu/Phoenix1.html>